

# NUMERICAL SOLUTION OF A SHOCK TUBE: A COMPARISON BETWEEN FORMULATIONS BASED ON THE SPLIT COEFFICIENT MATRIX METHOD

Tobias R. Gessner, [tobias@polo.ufsc.br](mailto:tobias@polo.ufsc.br)

Jader R. Barbosa Jr., [jrb@polo.ufsc.br](mailto:jrb@polo.ufsc.br)

Polo – Laboratórios de Pesquisa em Refrigeração e Termofísica

Departamento de Engenharia Mecânica, Universidade Federal de Santa Catarina, Florianópolis, SC, 88040-900, Brasil.

**Abstract.** Since it is amenable to analytical solutions, the single-phase shock tube problem has been continuously employed as a benchmark for the evaluation of numerical methods. The hyperbolic nature of the mass, momentum and energy conservation equations gives rise to discontinuities in the solution domain, such as shock and rarefaction waves, as well as contact discontinuities. In the present paper, numerical routines have been developed and validated via the finite differences based Split Coefficient Matrix (SCM) Method according to three distinct formulations: 1<sup>st</sup> order non-conservative, 1<sup>st</sup> order conservative and 2<sup>nd</sup> order conservative. The numerical results of the single phase shock tube simulations are compared with the analytical solution and evaluated with respect to the computational cost and occurrence of numerical diffusion and dispersion.

*Keywords:* Shock tube, hyperbolic PDE, Split Coefficient Matrix.

## 1. INTRODUCTION

The Split Coefficient Matrix Method (SCM), proposed by Chakravarthy et al. (1980), is a variation of the Method of Characteristics. Both are upwind schemes based on an algebraic manipulation of the eigenvalues and eigenvectors of the governing system of hyperbolic PDEs which enables the evaluation of the influence of the different mechanisms by which perturbations are propagated in the flow field (shock and rarefaction waves, advection, etc.). The technique has been developed initially for compressible single-phase flows, but was subsequently extended to two-phase flow problems (Romstedt, 1987). It can be formulated as a function of conservative and non-conservative variables, implicitly or explicitly.

The single-phase shock tube is a classical fluid dynamics problem which is governed by a set of hyperbolic PDEs. Shock tubes are widely employed in the study of high velocity compressible flows and in the measurement of chemical and thermodynamic properties of gases at high temperatures. Under certain assumptions, the single-phase shock tube model is amenable to analytical solution, as detailed in Anderson (1982). For this reason, it is frequently adopted as a benchmark for numerical solution schemes.

The present paper advances the first steps towards the consolidation of a research programme dedicated to the simulation of single-phase and two-phase transient flows via numerical methodologies developed for hyperbolic systems of equations (Städtke, 2006). In this communication, we develop numerical procedures based on the SCM method and to explore the usage of different variables and discretization schemes of the spatial derivatives via three distinct formulations: 1<sup>st</sup> order non-conservative, 1<sup>st</sup> order conservative and 2<sup>nd</sup> order conservative. The numerical methodologies are validated through a comparison with the analytical results of a single-phase shock tube.

## 2. MODELLING

The single-phase gas shock tube is composed of two horizontal chambers, separated by a diaphragm, as shown in Fig. 1. Methane ( $\text{CH}_4$ ), initially at rest, fills both cavities which are at the same uniform temperature, but at different pressure levels. As the diaphragm is removed, a transient flow of gas is initiated in the direction of the low pressure end of the shock tube.

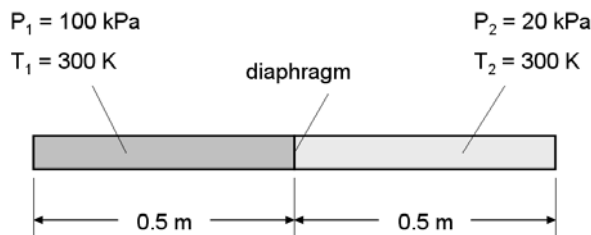


Figure 1. Problem geometry and initial conditions.

The flow is considered one-dimensional, inviscid and adiabatic. The hyperbolic system of equations resulting from the application of these hypotheses on the differential forms of the mass, linear momentum and energy equations is

given by Eqs. (1) to (3). The same hypotheses have been adopted in the analytical treatment of the problem (Anderson, 1982), so that a direct comparison between the numerical and analytical solutions is in order.

$$\frac{\partial \rho}{\partial t} + \frac{\partial}{\partial x}(\rho U) = 0 \quad (1)$$

$$\frac{\partial}{\partial t}(\rho U) + \frac{\partial}{\partial x}(\rho U^2) + \frac{\partial P}{\partial x} = 0 \quad (2)$$

$$\frac{\partial}{\partial t} \left[ \rho \left( e + \frac{U^2}{2} \right) \right] + \frac{\partial}{\partial x} \left[ \rho U \left( h + \frac{U^2}{2} \right) \right] = 0 \quad (3)$$

With the help of fundamental thermodynamic relations (Gyftopoulos and Beretta, 2005), Eqs. (1) to (3) can be re-written in terms of the non-conservative variables  $P$  (pressure),  $U$  (velocity) and  $s$  (specific entropy) as follows

$$\frac{\partial P}{\partial t} + U \frac{\partial P}{\partial x} + \rho c_s^2 \frac{\partial U}{\partial x} = 0 \quad (4)$$

$$\frac{\partial U}{\partial t} + U \frac{\partial U}{\partial x} + \frac{1}{\rho} \frac{\partial P}{\partial x} = 0 \quad (5)$$

$$\frac{\partial s}{\partial t} + U \frac{\partial s}{\partial x} = 0 \quad (6)$$

where  $c_s$  is the local sound velocity.

### 3. CONSERVATION EQUATIONS

#### 3.1. Non-conservative formulation

Equations (4) to (6) can be re-arranged in the compact form

$$\frac{\partial \vec{U}}{\partial t} + \mathbf{G} \frac{\partial \vec{U}}{\partial x} = 0 \quad (7)$$

where

$$\vec{U} = [P \quad U \quad s]^T \quad (8)$$

$$\mathbf{G} = \begin{bmatrix} U & \rho c_s^2 & 0 \\ \frac{1}{\rho} & U & 0 \\ 0 & 0 & U \end{bmatrix} \quad (9)$$

The coefficient matrix  $\mathbf{G}$  can be written in terms of the diagonal matrix containing the eigenvalues  $\mathbf{\Lambda}$ , the matrix with the eigenvectors arranged into columns  $\mathbf{T}$  and its inverse  $\mathbf{T}^{-1}$ , as follows,

$$\mathbf{G} = \mathbf{T} \mathbf{\Lambda} \mathbf{T}^{-1} \quad (10)$$

where

$$\mathbf{\Lambda} = \begin{bmatrix} \lambda_1 & 0 & 0 \\ 0 & \lambda_2 & 0 \\ 0 & 0 & \lambda_3 \end{bmatrix} = \begin{bmatrix} U + c_s & 0 & 0 \\ 0 & U - c_s & 0 \\ 0 & 0 & U \end{bmatrix} \quad (11)$$

$$\mathbf{T} = \begin{bmatrix} 1 & 1 & 0 \\ 1 & -1 & 0 \\ \rho c_s & -\rho c_s & 0 \\ 0 & 0 & 1 \end{bmatrix} \quad (12)$$

For subsonic flows, such as the present problem, the eigenvalues  $\lambda_1$  and  $\lambda_2$  represent the velocities with which any perturbation in  $U$  or  $P$  are propagated: the first is always positive and propagates the perturbation in the positive  $x$  direction; the second is always negative and propagates the perturbation in the negative  $x$  direction. The eigenvalue  $\lambda_3$ , in turn, indicates that any perturbation in the variable  $s$  is propagated at the local flow velocity  $U$ , which can be in the positive or negative  $x$  directions. The matrix of eigenvalues can be decomposed in three terms corresponding to  $\lambda_1$ ,  $\lambda_2$  and  $\lambda_3$  as follows,

$$\mathbf{G} = \mathbf{T}\mathbf{\Lambda}_1\mathbf{T}^{-1} + \mathbf{T}\mathbf{\Lambda}_2\mathbf{T}^{-1} + \mathbf{T}\mathbf{\Lambda}_3\mathbf{T}^{-1} = \mathbf{G}_1 + \mathbf{G}_2 + \mathbf{G}_3 \quad (13)$$

The so-called  $\mathbf{G}^+$  matrix can be constructed from the coefficients involved in the propagation in the positive  $x$  direction. Analogously, the  $\mathbf{G}^-$  matrix describes the propagation of perturbations in the flow properties in the negative  $x$  direction,

$$\mathbf{G}^+ = \mathbf{G}_1 + \max\left(\frac{U}{|U|}, 0\right)\mathbf{G}_3 \quad (14)$$

$$\mathbf{G}^- = \mathbf{G}_2 + \min\left(\frac{U}{|U|}, 0\right)\mathbf{G}_3 \quad (15)$$

Thus, Eq. (7) can be re-written as,

$$\frac{\partial \vec{U}}{\partial t} + \mathbf{G}^+ \frac{\partial \vec{U}}{\partial x} + \mathbf{G}^- \frac{\partial \vec{U}}{\partial x} = 0 \quad (16)$$

### 3.2. Conservative formulation

Based on Eqs. (1) to (3), the vector containing the unknown variables of the conservative formulation  $\vec{V}$  can be written as,

$$\vec{V} = \left[ \rho \quad \rho U \quad \rho \left( e + \frac{U^2}{2} \right) \right]^T = [\rho \quad G \quad E]^T \quad (17)$$

Thus, the re-parameterization of Eq. (7) gives,

$$\frac{\partial \vec{V}}{\partial t} + \mathbf{H} \frac{\partial \vec{V}}{\partial x} = 0 \quad (18)$$

where

$$\mathbf{H} = \mathbf{J}\mathbf{G}\mathbf{J}^{-1} \quad (19)$$

$$\mathbf{J} = \frac{\partial \vec{V}}{\partial \vec{U}} \quad (20)$$

The decomposition of the coefficient matrix  $\mathbf{H}$  is analogous to the decomposition of  $\mathbf{G}$  described in Section 3.1.

## 4. NUMERICAL IMPLEMENTATION

### 4.1. Non-conservative, 1<sup>st</sup> order finite differences

In the context of the numerical solution via finite differences, it seems sensible to evaluate the spatial derivative associated with  $\mathbf{G}^+$  (propagation in the positive direction) according to a Backward Differentiation Scheme (BDS) and that associated with  $\mathbf{G}^-$  (propagation in the negative direction) according to a Forward Differentiation Scheme (FDS). An implicit formulation of the governing equations gives,

$$\frac{\bar{U}_i - \bar{U}_i^0}{\Delta t} + \mathbf{G}^+ \frac{\bar{U}_i - \bar{U}_{i-1}}{\Delta x_i} + \mathbf{G}^- \frac{\bar{U}_{i+1} - \bar{U}_i}{\Delta x_{i+1}} = 0 \quad (21)$$

where  $\Delta x_i = x_i - x_{i-1}$ . Eq. (21) can be cast in the more convenient form,

$$\mathbf{A}\bar{X} = \bar{K} \quad (22)$$

where  $\mathbf{A}$  is a tri-diagonal block matrix whose non-zero elements are sub-matrices given by,

$$A_{ii-1} = -\frac{1}{\Delta x_i} \mathbf{G}^+ \quad (23)$$

$$A_{ii} = \frac{1}{\Delta t} \mathbf{I} + \frac{1}{\Delta x_i} \mathbf{G}^+ - \frac{1}{\Delta x_{i+1}} \mathbf{G}^- \quad (24)$$

$$A_{ii+1} = \frac{1}{\Delta x_{i+1}} \mathbf{G}^- \quad (25)$$

and

$$X_i = [P_i \quad U_i \quad s_i]^T \quad (26)$$

$$K_i = \left[ \begin{array}{ccc} P_i^0 & U_i^0 & s_i^0 \\ \Delta t & \Delta t & \Delta t \end{array} \right]^T \quad (27)$$

### 4.2. Conservative, 1<sup>st</sup> order finite differences

A procedure analogous to the one described in Section 4.1 renders Eq. (18) in the following form,

$$\frac{\bar{V}_i - \bar{V}_i^0}{\Delta t} + \mathbf{H}^+ \frac{\bar{V}_i - \bar{V}_{i-1}}{\Delta x_i} + \mathbf{H}^- \frac{\bar{V}_{i+1} - \bar{V}_i}{\Delta x_{i+1}} = 0 \quad (28)$$

where the linear system corresponding to Eq. (28) can also be cast in the form of Eq. (22).

### 4.3. Conservative, 2<sup>nd</sup> order finite differences

When 2<sup>nd</sup> order BDS and FDS schemes are employed, the discretized form of Eq. (18) becomes

$$\frac{\bar{V}_i - \bar{V}_i^0}{\Delta t} + \mathbf{H}^+ \left[ \frac{(\beta^2 - 1)\bar{V}_i - \beta^2\bar{V}_{i-1} + \bar{V}_{i-2}}{(\beta^2 - \beta)\Delta x_i} \right] - \mathbf{H}^- \left[ \frac{(\varphi^2 - 1)\bar{V}_i - \varphi^2\bar{V}_{i+1} + \bar{V}_{i+2}}{(\varphi^2 - \varphi)\Delta x_{i+1}} \right] = 0 \quad (29)$$

where

$$\beta = \frac{\Delta x_i + \Delta x_{i-1}}{\Delta x_i}, \quad \varphi = \frac{\Delta x_{i+1} + \Delta x_{i+2}}{\Delta x_{i+1}} \quad (30)$$

Once again, it is possible to write Eq. (29) in the form  $\mathbf{A}\vec{X} = \vec{K}$ , where

$$A_{ii-2} = \frac{1}{(\beta^2 - \beta)\Delta x_i} \mathbf{H}^+ \quad (31)$$

$$A_{ii-1} = -\frac{\beta^2}{(\beta^2 - \beta)\Delta x_i} \mathbf{H}^+ \quad (32)$$

$$A_{ii} = \frac{1}{\Delta t} \mathbf{I} + \frac{\beta^2 - 1}{(\beta^2 - \beta)\Delta x_i} \mathbf{H}^+ - \frac{\varphi^2 - 1}{(\varphi^2 - \varphi)\Delta x_{i+1}} \mathbf{H}^- \quad (33)$$

$$A_{ii+1} = \frac{\varphi^2}{(\varphi^2 - \varphi)\Delta x_{i+1}} \mathbf{H}^- \quad (34)$$

$$A_{ii+2} = -\frac{1}{(\varphi^2 - \varphi)\Delta x_{i+1}} \mathbf{H}^- \quad (35)$$

At the second node, however, only the 1<sup>st</sup> order BDS scheme can be applied due to the existence of only one node at its left. Similarly, at the next-to-last node, only the 1<sup>st</sup> order FDS scheme can be applied due to the existence of only one node at its right. In both cases, the coefficients of the matrix  $\mathbf{A}$  corresponding to such nodes are modified accordingly.

#### 4.4. Boundary conditions

It is assumed that the properties at the left end are influenced only by the propagation associated with the negative eigenvalues. Likewise, the properties at the right end are assumed to be influenced only by the propagation associated with the positive eigenvalues. At these points (nodes), the flow velocity and the mass flux  $G$  are set to zero, which results in a modification of the coefficients of the matrix  $\mathbf{A}$  associated with the momentum conservation equation at those two points.

#### 4.5. Computational grid and solution procedure

The same computational grid has been utilized in the three cases, which consists of 501 equally spaced (2 mm) nodes. The time step  $\Delta t$  was set at 1  $\mu$ s. The solution procedure, at each time step, consists of the following stages:

1. All fields are set equal to the converged values obtained at the previous time step;
2. The vector  $\vec{K}$  is calculated;
3. The eigenvalues are calculated at each node;
4. The coefficients of the matrix  $\mathbf{A}$  are calculated;
5. The system of equations given by Eq. (22) is solved using the GBAND algorithm (Aziz and Settari, 1979; Ouyang, 1998), and new values of  $P$ ,  $U$  and  $s$  (non-conservative formulation), or  $\rho$ ,  $G$  and  $E$  (conservative formulation) are calculated;
6. Based on the latest fields of  $P$  and  $s$  (non-conservative formulation) or of  $\rho$  and  $e$  (conservative formulation), the remaining thermodynamic properties are calculated at each node using the equation of state available in the Fortran source of the REFPROP 7.0 package (Lemmon et al., 2002);
7. If the convergence criterion is not met, return to stage 3. The convergence criterion has been established based on the absolute difference between the values of each variable at two successive iterations (see Table 1 for the tolerances applied to each variable).

Table 1. Tolerances associated with each variable.

Formulation	Variable	Tolerance
Non-conservative	$P$ [kPa]	$1 \times 10^{-4}$
	$U$ [m/s]	$1 \times 10^{-4}$
	$s$ [kJ/kgK]	$1 \times 10^{-4}$
Conservative	$\rho$ [kg/m <sup>3</sup> ]	$1 \times 10^{-4}$
	$G$ [kg/m <sup>2</sup> s]	$1 \times 10^{-1}$
	$E$ [kJ/m <sup>3</sup> ]	$1 \times 10^{-1}$

## 5. RESULTS

If the gas in the shock tube behaves as a perfect gas, then the problem is amenable to analytical solution, as presented in detail in Chapter 7 of Anderson (1982). Those results have been utilized to validate the three formulations put forward in the present work.

As can be seen from Figs. 2 to 5, the pressure, velocity, density and temperature predictions change very little when the conservative formulation is replaced by a non-conservative formulation. This, in association with the fact that the coefficient matrix  $\mathbf{G}$  is substantially simpler than the matrix  $\mathbf{H}$  (which results in less computational effort), makes the non-conservative formulation more advantageous in this particular case. The discontinuities observed in the numerical predictions of the flow properties are clearly non-physical and can be attributed to numerical diffusion effects which are typical of 1<sup>st</sup> order interpolation schemes.

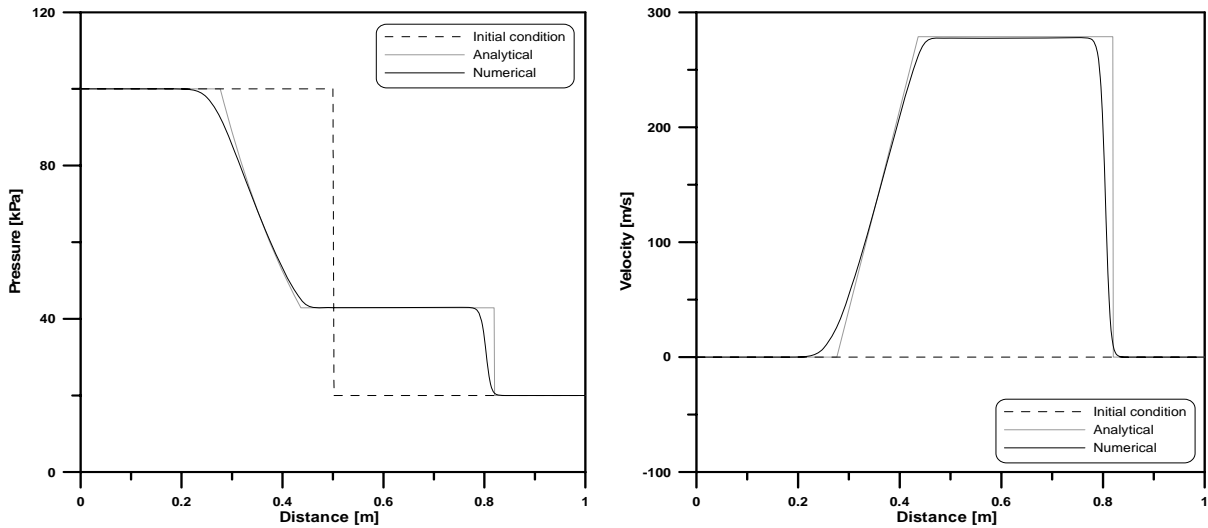


Figure 2. Pressure and velocity fields at 500  $\mu\text{s}$ : 1<sup>st</sup> order non-conservative formulation.

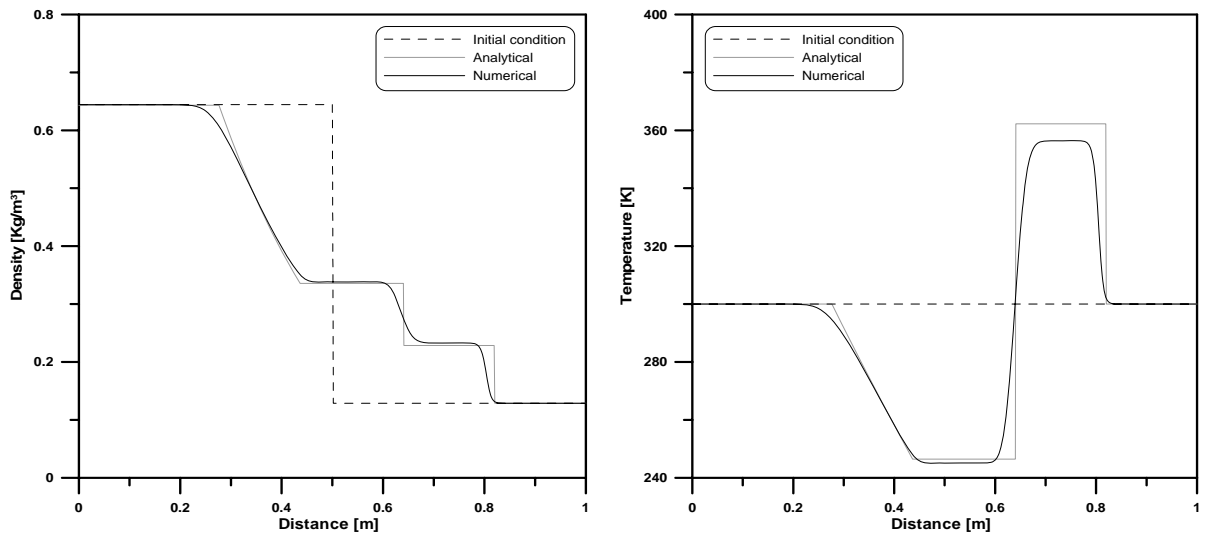


Figure 3. Density and temperature fields at 500  $\mu\text{s}$ : 1<sup>st</sup> order non-conservative formulation.

Figures 6 and 7 show the predictions of pressure, velocity, density and temperature obtained with the 2<sup>nd</sup> order conservative formulation. As can be seen, the numerical predictions are quite encouraging despite the instabilities observed near the discontinuities. This can be attributed to numerical dispersion effects, which are typical of such a type of interpolation scheme. However, as shown in Table 2, the predictions of the 2<sup>nd</sup> order formulation are closer to the exact solution than those obtained with the 1<sup>st</sup> order formulations.

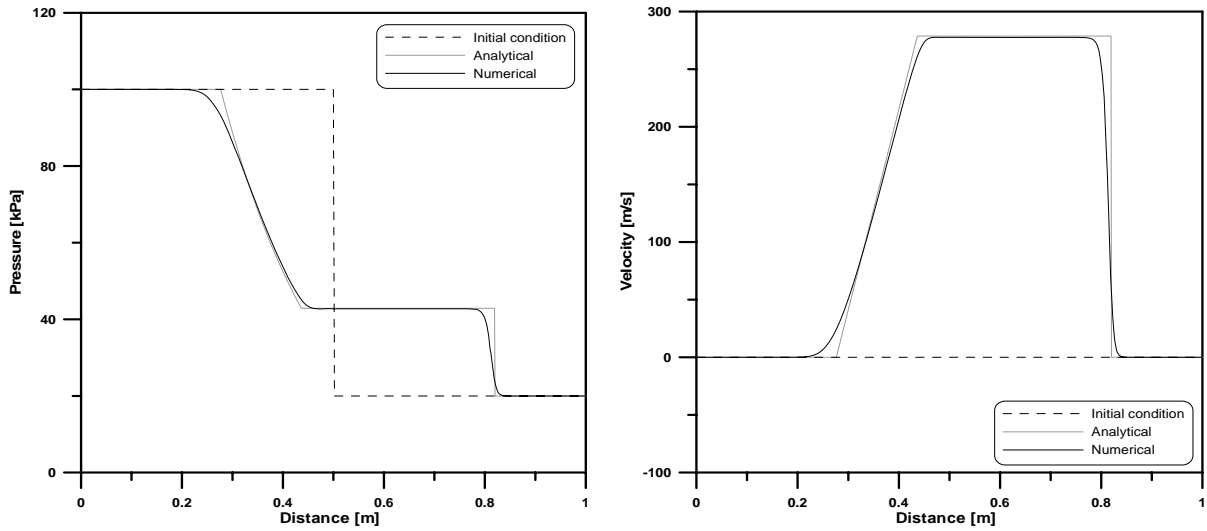


Figure 4. Pressure and velocity fields at 500  $\mu$ s: 1<sup>st</sup> order conservative formulation.

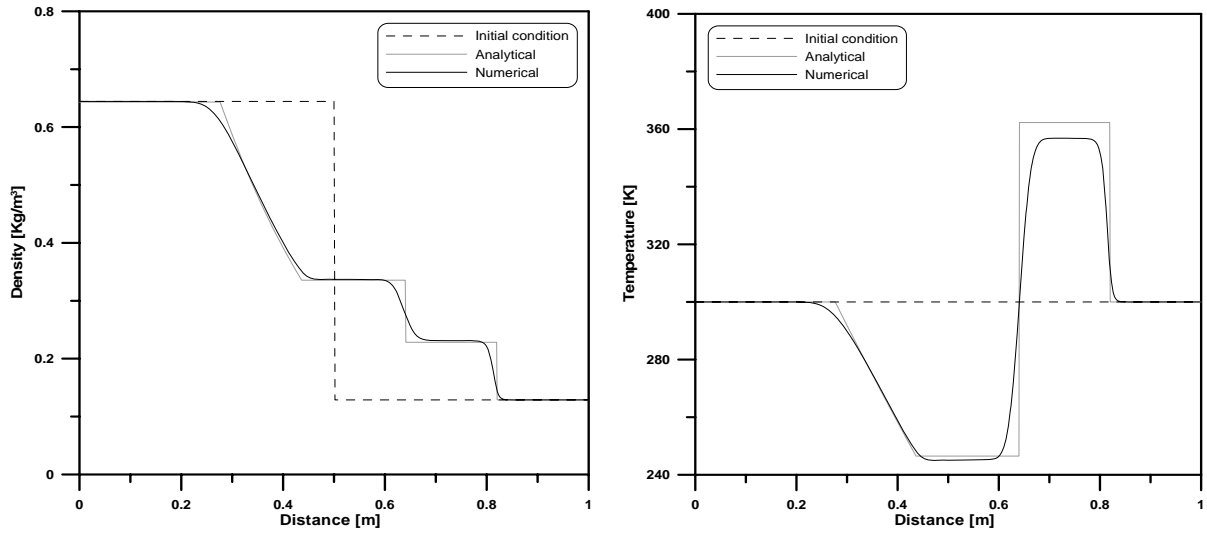


Figure 5. Density and temperature fields at 500  $\mu$ s: 1<sup>st</sup> order conservative formulation.

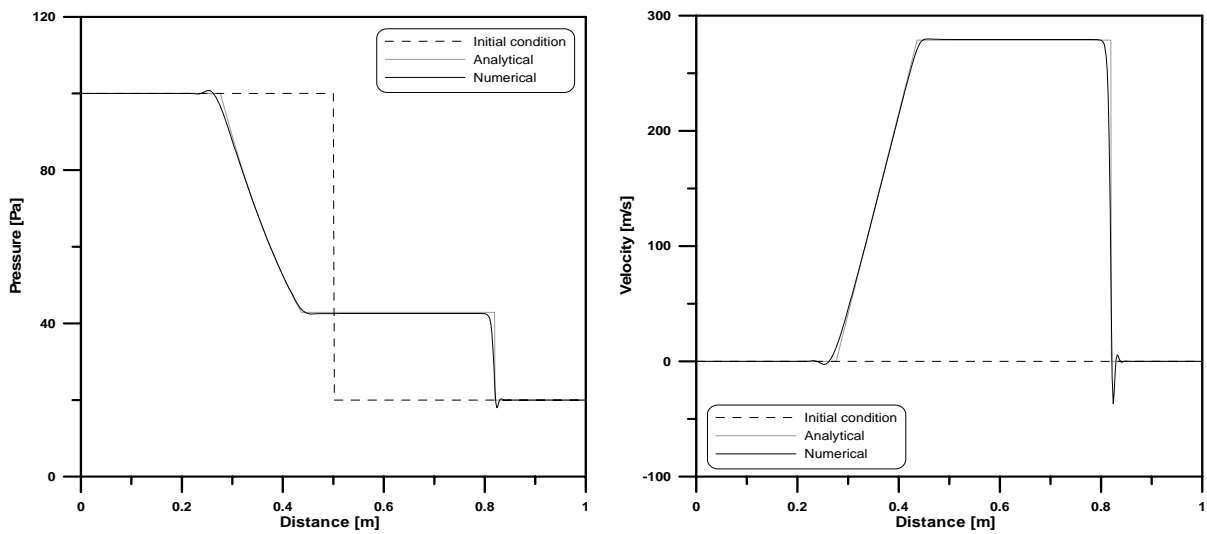


Figure 6. Pressure and velocity fields at 500  $\mu$ s: 2<sup>nd</sup> order conservative formulation.

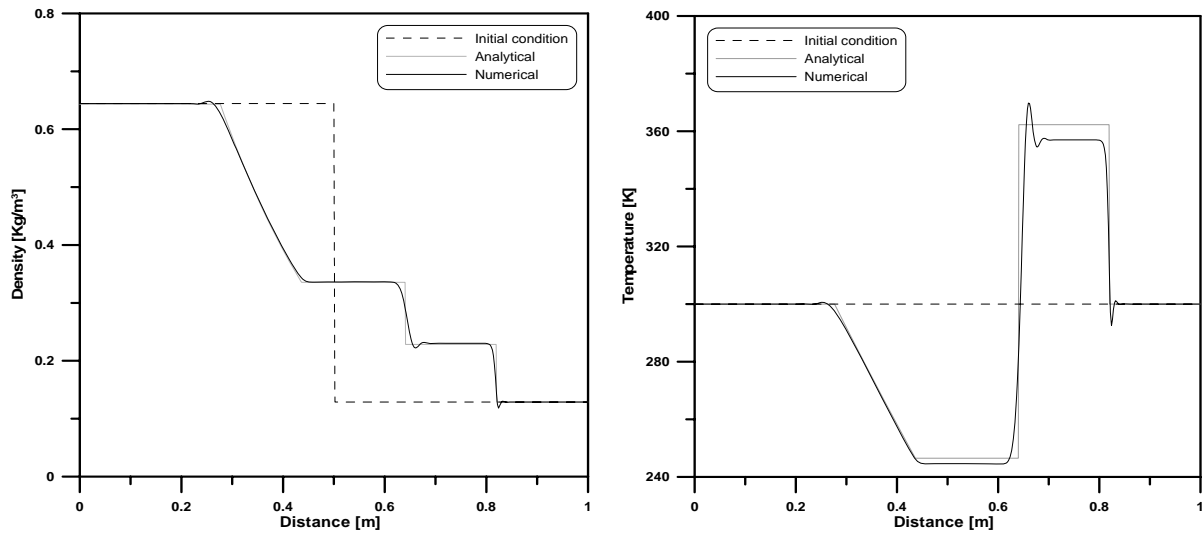


Figure 7. Density and temperature fields at 500  $\mu$ s: 2<sup>nd</sup> order conservative formulation.

Table 2. Summary of the numerical predictions at 500  $\mu$ s.

Formulation	Average error				Computational time [s]
	Pressure [kPa]	Velocity [m/s]	Temperature [K]	Density [kg/m <sup>3</sup> ]	
1 <sup>st</sup> order NC	0.80	0.0016	3.0	0.011	45.2
1 <sup>st</sup> order C	0.67	0.0013	3.3	0.0053	76.6
2 <sup>nd</sup> order C	0.32	0.00063	1.9	0.0024	115

The overall computational time is also shown in Table 2 for the three formulations. It should be borne in mind that the actual calculation of the physical properties via the equation of state (Lemmon et al., 2002), carried out at each iteration, takes up a significant fraction of the computational time (more than 90%).

## 6. CONCLUSIONS

In the present paper, numerical routines based on the SCM method have been developed based on three different formulations: 1<sup>st</sup> order non-conservative, 1<sup>st</sup> order conservative and 2<sup>nd</sup> order conservative. The methodology has been validated through a comparison with the analytical solution of a single-phase shock tube (Anderson, 1982). It was concluded that, for the present problem, equally satisfactory results can be obtained with conservative and non-conservative formulations. Furthermore, it was observed that the 1st order interpolation schemes give rise to numerical diffusion in the vicinity of the discontinuities, whereas the 2<sup>nd</sup> order schemes are associated with the appearance of numerical dispersion effects. The numerical results obtained with the 2<sup>nd</sup> order scheme were the closest to the analytical solutions.

## 7. REFERENCES

- Anderson, J. D.; 1982, "Modern Compressible Flow". McGraw-Hill, NY.
- Aziz, K., Settari, A., 1979, "Petroleum Reservoir Engineering", Elsevier Applied Science, New York, NY.
- Chakravarthy, S. R., Andersen, D. A., Salas, M. D.; 1980, "The Split Coefficient Matrix Method for Hyperbolic Systems of Gasdynamic Equations". AIAA 18<sup>th</sup> Science Meeting, paper 80-0268, Pasadena, CA.
- Gyftopoulos, E. P., Beretta, G. P., 2005, "Thermodynamics: Foundations and Applications", Dover, NY.
- Lemmon, E.W., McLinden, M.O, Huber, M.L., 2002, REFPROP V. 7.0, NIST.
- Ouyang, L.-B.; 1998, "Single Phase and Multiphase Flow in Horizontal Wells". PhD thesis, Dept. of Petroleum Engineering, Stanford University, Stanford, CA
- Städtke, H.; 2006, "Gasdynamic Aspects of Two-Phase Flow". Wiley-VCH.
- Romstedt, P.; 1987, "A Split-Matrix Method for the Numerical Solution of Two-Phase Flow Equations". Int. Top. Meeting on Advances in Reactor Physics, Mathematics and Computation, Paris, France.

## 8. RESPONSIBILITY NOTICE

The authors are the only responsible for the printed material included in this paper.